Journal of Environmental Management 395 (2025) 127815

Contents lists available at ScienceDirect

Journal of Environmental Management

journal homepage: www.elsevier.com/locate/jenvman

Research article

Drivers of biocapacity and global impact of the world's largest mangrove in ecological footprint accounting

Md Rezaul Karim [a,**], Md Shamim Reza Saimun [b], Hossain Mahmud Sammi [b,c], Ariful Khan [b], Md Sahinur Islam Fahim [b,d], Fahmida Sultana [b,e], Sanjeev K. Srivastava [f], Pallab Mozumder [g,h], Daniel A. Friess [i], Sharif A. Mukul [f,h,j], Mohammed A.S. Arfin-Khan [b,*]

[a] Institute of Forestry and Conservation, John H. Daniels Faculty of Architecture, Landscape, and Design, University of Toronto, 33 Willcocks Street, Toronto, ON M5S 3B3, Canada
[b] Department of Forestry and Environmental Science, School of Agriculture and Mineral Sciences, Shahjalal University of Science and Technology, Sylhet 3114, Bangladesh
[c] Department of Biology, Georgia Southern University, Statesboro, GA 30458, USA
[d] Department of Food and Resource Economics, University of Copenhagen, DK-1958, Denmark
[e] School of Biosciences, Geography and Physics, Faculty of Science and Engineering, Swansea University, Singleton Park Swansea SA2 8PP Wales, UK
[f] School of Science, Technology and Engineering (SSTE), University of the Sunshine Coast, Maroochydore DC, Queensland 4556, Australia
[g] Department of Economics, Florida International University, Miami, FL 33199, USA
[h] Department of Earth and Environment, Florida International University, Miami, FL 33199, USA
[i] Department of Earth and Environmental Sciences, Tulane University, New Orleans, LA 70118, USA
[j] Department of Environment and Development Studies, United International University, Dhaka 1212, Bangladesh

ARTICLE INFO

Keywords:
Mangrove
The Sundarbans
Climate change
Salinity
Biocapacity
Ecosystem services
Ecological footprint accounting
Spatial modeling

ABSTRACT

Mangrove forests play a vital role in climate regulation, carbon storage, and biodiversity conservation, yet their capacity to meet ecological demands remains poorly quantified. The Sundarbans, the world's largest contiguous mangrove ecosystem, faces escalating environmental pressures that threaten its biocapacity—the ability of ecosystems to provide renewable resources and absorb human-generated waste. This study evaluates biocapacity and ecological deficit/reserve at local, national, and global scales by integrating key environmental drivers, including salinity, stand structure, and climate variables. Data were collected from 54 georeferenced plots covering 54 management compartments, and analyses were conducted at plot-level, compartment-level, and broader regional scales. Results reveal significant spatial variability, with the oligohaline zone supporting the largest ecological reserve (1.87 ± 0.164 gha/person), followed by the mesohaline (1.13 ± 0.167 gha/person), whereas polyhaline regions exhibit the lowest reserve (0.48 ± 0.1 gha/person). Globally, polyhaline zones face severe ecological deficits (−1.11 ± 0.1 gha/person), highlighting their vulnerability to environmental stressors. Biocapacity correlates with salinity ($r = -0.39$), temperature ($r = -0.42$), precipitation ($r = 0.32$), and elevation ($r = 0.35$), while structural attributes such as tree height ($r = 0.33$) and wood density ($r = 0.34$) further shape ecosystem capacity. To strengthen environmental management, biocapacity assessments should be integrated into policy and conservation planning frameworks for sustainable resource allocation. As climate change alters temperature and salinity regimes, proactive mitigation strategies, ecosystem-based adaptation, and sustainable management practices are essential for maintaining ecological balance, reducing biodiversity loss, and ensuring the stability of mangrove ecosystem services.

1. Introduction

Rapid resource exploitation and growing demands driven by population and economic pressures have severely impacted forest biocapacity (Kumar et al., 2022; Sarkodie, 2021). This has intensified the need for sustainable frameworks, as biocapacity—reflecting the capacity

** Corresponding author.
* Corresponding author.
E-mail addresses: rezaul.karim@mail.utoronto.ca (M.R. Karim), khan-for@sust.edu (M.A.S. Arfin-Khan).

https://doi.org/10.1016/j.jenvman.2025.127815
Received 9 March 2025; Received in revised form 1 October 2025; Accepted 25 October 2025
Available online 30 October 2025

of ecosystems to generate renewable resources and absorb wastes—is increasingly strained (Niccolucci et al., 2012). To address this, ecosystem-based management (EBM) and global initiatives like REDD+ are essential for mitigating ecological degradation, reducing the global ecological footprint, and enhancing biomass carbon storage (Angelsen et al., 2018; Zaman, 2022; Patel et al., 2024). Central to this context are the concepts of biocapacity, introduced by Wackernagel and Rees, (1996) as a measure of an ecosystem's regenerative ability, and the ecological footprint, which quantifies human demand on that capacity. The relationship between these two metrics is crucial for understanding sustainability (Monfreda et al., 2004; Dworatzek et al., 2024).

Among forest ecosystems, mangroves are particularly significant, covering approximately 14.5 million hectares globally (Jia et al., 2023). Growing in intertidal zones, mangroves provide a range of wood and non-wood products while performing essential environmental functions (FAO, 2020). Mangroves provide critical ecological services, including biodiversity, stabilize shorelines, filter water, and sequester carbon, collectively underpinning key ecosystem services critical to human and ecological well-being (Donato et al., 2011). Biomass productivity, which largely drives these services, increases with age but is highly sensitive to environmental factors such as climate, soil conditions, and stand structures (Barr et al., 2013; Zheng and Takeuchi, 2022; Zheng et al., 2023; Panda et al., 2024).

These vital ecosystems are shaped by two dominant and interconnected drivers: climate change and human activities (Maina et al., 2021). Climate change intensifies challenges by shifting hydrological regimes, altering species distributions, increasing storm frequency, and causing sea-level rise, which exacerbates salinity intrusion (Akber et al., 2018; Banerjee et al., 2017; Friess et al., 2022; Chowdhury et al., 2024). Simultaneously, human-induced pressures, primarily deforestation for agriculture and aquaculture and unsustainable resource extraction, fragment habitats, diminish biomass, and accelerate ecological degradation (Sahavacharin et al., 2022; Guild et al., 2025). Increased salinity directly inhibits mangrove growth and biomass accumulation, reducing the ecosystem's capacity to generate renewable resources and absorb ecological impacts, thereby decreasing biological carrying capacity (Ahmed et al., 2022). Extreme weather events further damage canopy structure and alter hydrological regimes, compounding these effects on biocapacity (Howe et al., 2025). The severity of these combined pressures is underscored by the global decline of mangrove areas by 1.04 million hectares between 1990 and 2020, highlighting the urgent need for conservation efforts (Bunting et al., 2022).

Ongoing extensive research has focused on mangrove ecosystem services, carbon stocks, and productivity (Gilang Qur'ani et al., 2024; Gouvêa et al., 2022; Sharma et al., 2023; Tasneem and Ahsan, 2024; Twilley et al., 2017). However, despite increasing recognition of these threats, a critical knowledge gap remains. Lacking are comprehensive and integrated assessments that explicitly quantify the combined impacts of climate change and human-induced drivers on mangrove biocapacity and ecological deficits across different spatial scales. This gap is significant because such assessments are essential for informing ecosystem-based management and sustainability strategies under future environmental scenarios (Zheng et al., 2023).

This research gap is particularly evident in the Sundarbans, the largest contiguous mangrove forest globally, where existing studies primarily address carbon storage, biodiversity, and ecosystem services with limited attention given to biocapacity and ecological footprint (Bera et al., 2022; Iqbal, 2020; Islam et al., 2018).

Spanning over 10,000 km^2 in India and Bangladesh, the Sundarbans is a UNESCO World Heritage Site that constitutes 38.12 % of the forest area in Bangladesh (BFD, 2017). Rich in biodiversity, the Sundarbans hosts about 50 % of the world's mangrove plant species and supports approximately one million people who rely on it for resources such as fuelwood and fishing (Aziz and Paul, 2015; Mahmood et al., 2021). It also plays a critical role in protecting coastal communities from tidal surges and cyclones while preventing coastal erosion (Akber et al., 2018; Hale et al., 2019). Despite its significance, the Sundarbans faces ongoing pressures from land conversion for agriculture and aquaculture, rising sea levels, and increased salinity due to climate change (Chowdhury and Hafsa, 2022; Roy et al., 2024). These environmental stressors reduce mangrove productivity and ecosystem functioning, directly impacting biological carrying capacity and resource provision. Extreme weather events have further damaged mangrove areas, leading to a decline in biocapacity (Mandal and Hosaka, 2020). Nevertheless, the Sundarbans remains vital for regional economic stability and ecosystem health (Mahmood et al., 2021; Sarker et al., 2019).

Given the Sundarbans' critical role in carbon sequestration, coastal protection, and economic livelihoods, understanding its biocapacity is vital for developing effective conservation and management strategies at regional and global scales. Therefore, clarifying how climate change and human activities interactively drive changes in biocapacity and ecological reserve status can provide essential knowledge for safeguarding this vulnerable ecosystem. This study aims to fill this knowledge gap by assessing (a) the spatial response patterns of biocapacity to ecological footprint pressures across local, national, and global scales, and (b) the influence of soil conditions, stand structures, and climatic factors on biocapacity, along with its ecological reserve or deficit status. By integrating ecological footprint accounting with spatial modeling and statistical analyses, including spatial interpolation, principal component analysis, and regression modeling, the study provides a robust methodological framework. The expected outcomes will provide precise scientific evidence for developing zoning protection strategies, such as prioritizing the restoration of high-deficit hypersaline areas, and for guiding ecosystem-based adaptive management in the Sundarbans.

2. Methods

2.1. Study area

The Sundarbans, the largest contiguous mangrove forest in the world, spans the India Bangladesh border along the northern coastline of the Bay of Bengal. The Bangladesh portion, located between 89°00′ and 89°55′E and 21°30′–22°30′N (Fig. 1), covers 599,330 ha, representing approximately 62 % of the forest, with the remainder (426,300 ha) in West Bengal, India (Borrell et al., 2016). The Sundarbans is globally recognized as one of the most diverse and productive ecosystems, providing critical protection against cyclones, tidal flooding, erosion, and other natural disasters (Payo et al., 2016). During cyclones Sidr (2007), Aila (2009), and Amphan (2020), the Sundarbans acted as a buffer, safeguarding coastal populations (Mishra et al., 2021). The forest comprises approximately 200 islands separated by 400 tidal rivers and canals, with strong gradients in salinity, tidal influence, and soil properties, providing habitat complexity relevant to ecological assessments (Sen and Ghorai, 2019). Notable species include sundari (*Heritiera fomes*), goran (*Ceriops decandra*), gewa (*Excoecaria agallocha*), golpata (*Nypa fruticans*), keora (*Sonneratia apetala*), passur (*Xylocarpus mekongensis*), baen (*Avicennia officinalis*), and garjan (*Rhizophora mucronata*) (Islam et al., 2014). The Bangladesh portion of the Sundarbans is home to 45 % of the country's mammals, 42 % of its birds, 46 % of its reptiles, and 36 % of its amphibians with several endangered species, including the Bengal tiger (*Panthera tigris*), jungle cat (*Felis chaus*), estuarine crocodile (*Crocodylus porosus*), irrawaddy dolphin (*Orcaella brevirostris*), northern river terrapin (*Batagur baska*), and rock python (*Python molurus*) (Ahmed and Rahman, 2023). Approximately 2.5 million people live around the Sundarbans and rely directly on its resources for fuelwood, fishing, and small-scale agriculture (Gopal and Chauhan, 2018). These human pressures, together with climate change impacts such as rising sea levels and increasing salinity, reduce habitat quality and underscore the importance of assessing ecological deficits and surpluses across different zones.

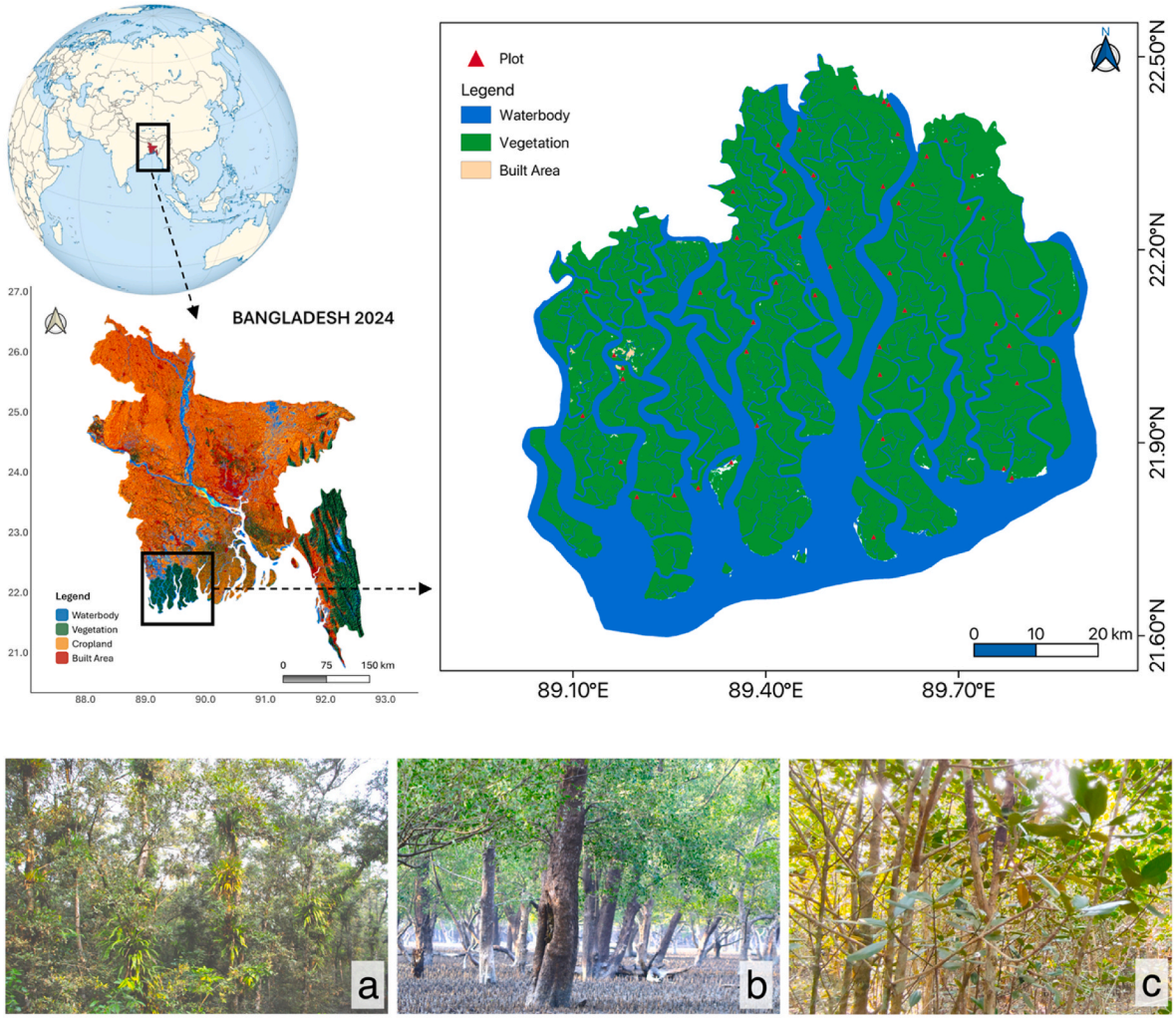

Fig. 1. Spatial distribution of study plots within the Sundarbans mangrove forest, southwestern Bangladesh. A total of 54 plots were established across 54 forest compartments, with representative imagery of key dominant species types: (a) *Heritiera fomes* (Sundri), (b) *Sonneratia apetala* (Keora), and (c) *Excoecaria agallocha* (Gewa) and/or *Avicennia officinalis* (Baen).

2.2. Plot selection and sampling design

A total of 54 plots were established within the Bangladesh Sundarbans, covering 54 forest compartments (the standard administrative and management units designated by the Bangladesh Forest Department) (Fig. 1). A systematic sampling design stratified by compartment was employed, with one plot established per compartment to ensure even spatial representation across the full extent of the study area. Within each compartment, plot locations were determined based on field accessibility, with all plots positioned at least 20 m inland from the nearest river channel to minimize edge effects associated with tidal influence and to ensure consistency in sampling terrestrial forest conditions. Plots were distributed systematically across salinity zones and elevation gradients to capture ecological variability, ensuring representativeness for multi-scale analysis. This placement also reflected practical considerations of field safety and logistical feasibility in a challenging mangrove environment. Each plot was standardized to 20 m × 20 m (400 m^2) in size, following established protocols for vegetation and ecological assessments in mangrove ecosystems.

2.3. Field data collection

Fieldwork was conducted from December 2021 to February 2022, during the most suitable period following the monsoon season, when vegetation remains actively growing and weather conditions are favorable for safe and efficient field surveys. During this time, the general characteristics of all plots were documented. Geographic coordinates and elevation at plot centers were recorded using a handheld GPS device (Garmin GPSMAP 67 series, Garmin, Switzerland), which features GPS and GLONASS positioning systems. Tree biomass data were collected non-destructively following the guidelines provided by Pearson et al. (2007) from 28 species (Supplement 1). All individual trees within each 20 m × 20 m plot with a diameter at breast height (DBH) ≥ 5 cm were censused, identified to species, and measured for DBH and height. For multi-stemmed trees, the diameter of each stem below breast height was measured separately. Tree height was determined using a Haga altimeter (Haga GMBH & Co., Nuremberg, Germany) by using following formulae (Eq. 1),

$$\text{Tree height} = \left(\frac{(\text{top crown reading} - \text{bottom reading}) \times \text{ground distance}}{100}\right) + 1.6\,\text{m} \quad \text{(Eq. 1)}$$

Here, ground distance was calculated through meter tape. Wood cores were collected at breast height (1.3 m), avoiding knots, with one core per stem, and were dried at 105 °C for 24 h following international wood density testing standards (Flores and Coomes, 2011). Tree species abundance was quantified by counting the number of individual trees

within each 400 m^2 plot. The count was then converted to a per hectare (ha) basis using the equation (Eq. 2),

$$\text{Abundance}\left(\text{individuals}\cdot\text{ha}^{-1}\right)=\frac{\text{Number of individuals}}{400\ \text{m}^2}\times 10,000\ \text{m}^2\Big/\text{ha} \quad \text{(Eq. 2)}$$

Species richness, defined as the total number of species within each plot, was similarly standardized to a per ha basis. Canopy cover was assessed using a crown densiometer (Spherical concave densiometer, Forestry Suppliers, US). Measurements were taken at four points within each plot, and the average percentage of canopy cover was calculated to estimate overall canopy density.

2.4. Field sample analysis

Wood density, soil pH, electrical conductivity, bulk density, litter organic carbon, and soil organic carbon were measured (Supplement 2). A non-destructive method was employed to estimate above-ground biomass (AGB) in tons per hectare. The following allometric equation, adapted from Chave et al. (2014), was utilized (Eq. 3):

$$\text{AGB}=\exp\left(-2.977+\ln\left(\rho\cdot D^2\cdot H\right)\right) \quad \text{(Eq. 3)}$$

where AGB is the above-ground biomass (kg), ρ is the wood density (g/cm^3), D is the diameter at breast height (1.3m) in cm, and H is the height of the tree in meters.

The biocapacity of biomass production (BCB) was calculated using a modified equation (Eq. 4) from Monfreda et al. (2004):

$$\text{BC}_\text{B}=\frac{\text{YF}_\text{B}\cdot\text{EQF}_\text{B}}{\text{P}} \quad \text{(Eq. 4)}$$

where BC_B represents the biocapacity of biomass production (global hectare) per person (gha/person), YF_B is the yield factor, and EQF_B is the equivalence factor for biomass production. The yield factor was derived as the ratio between local biomass production per hectare and the global forest biomass production, using data from the Global Forest Resources Assessment (FAO, 2020). The equivalence factor for biomass production was obtained from the National Footprint Accounts (FDF, 2023). The local plot wise population data, P was collected from the Government of Bangladesh Census Report (BBS, 2022).

2.5. Estimation of the ecological footprint of biomass production

The ecological footprint of biomass production was assessed at both local and national level. For local biomass, the following equation (Eq. 5) was applied:

$$\text{EF}_{\text{B(L)}}=\left(\frac{\text{P}_{\text{B(L)}}}{\text{Y}_\text{B}}\right)\cdot\text{EQF}_\text{B} \quad \text{(Eq. 5)}$$

where $EF_{B(L)}$ is the Ecological Footprint of local biomass (global hectare) per person (gha/person), $P_{B(L)}$ is the average local biomass harvest, Y_B is the global average yield of harvestable biomass, and EQF_B is the equivalence factor. Local footprint biomass data were sourced from the local government inventory report (GoB, 2019), while the national ($EF_{B(N)}$) and global ($EF_{B(G)}$) average was derived from the updated dataset of Global Footprint Network (GFN) database (Lo et al., 2025).

2.6. Estimation of the ecological deficit/reserve on local, national and global level

Estimation of ecological deficit and reserve at local, national, and global levels was conducted using a subtraction method. The net ecological reserve or deficit was calculated by subtracting the ecological footprint of biomass production from the biocapacity (gha/person) at each respective scale. The calculation was performed using the following equation (Eq. 6):

$$\text{Ecological deficit/reserve}=\text{BC}_\text{B}-\text{EF}_{\text{B(L)}}/\text{EF}_{\text{B(N)}}/\text{EF}_{\text{B(G)}} \quad \text{(Eq. 6)}$$

In this equation, a positive value indicates an ecological reserve, while a negative value signifies an ecological deficit.

2.7. Spatial biocapacity mapping using ordinary kriging

Biocapacity data were collected at the plot level from 54 locations across the Sundarbans mangrove forest, and ecological deficit and reserve data were compiled and analyzed at local, national, and global scales. Spatial dependence was evaluated through variogram modeling, with the variogram fitted using a linear model and specific adjustments made for partial sill, range, and nugget parameters to accurately capture spatial correlation. This approach facilitates precise spatial assessments critical for ecosystem monitoring and management. The entire workflow, encompassing variogram modeling, kriging, and visualization, was automated using a custom function based on the methodology outlined by Oliver & Webster (2014) using a 400×400 grid, ensuring detailed spatial coverage. The study area boundaries were defined using a shapefile, and all interpolations were masked to prevent extrapolation beyond these boundaries. Spatial operations were executed using the '*gstat*', '*sf*', '*raster*', and '*sp*' libraries in R version 4.4.1 (R Core Team, 2024). Visualization of the interpolated results was performed with *ggplot2*, employing a custom color scale to enhance clarity. High-resolution maps, displaying the spatial distribution of biocapacity (in global hectares per person), were generated and saved as PNG files. This methodological approach provided a comprehensive spatial analysis of biocapacity and ecological deficit/reserve within the Sundarbans, offering insights into the spatial variability and the influence of environmental and anthropogenic factors on this critical ecosystem.

2.8. Salinity zone and related climatic data collection

The study encompassed 54 plots distributed across three major salinity zones. Based on soil salinity distribution from our electric conductivity soil parameters, three distinct zones were identified: oligohaline (salinity <2 mS cm^{-1}), mesohaline (salinity 2–4 mS cm^{-1}), and polyhaline (salinity >4 mS cm^{-1}) (Siddique, 2001). Detailed of the plot number and associated salinity zone are provided in Supplement 3. In addition, climatic data, including mean annual temperature (°C), total annual precipitation (mm), and mean annual wind speed (m/s), were obtained from the WorldClim version 2.1 dataset at a 1 km spatial resolution. This dataset provides high-resolution gridded climate surfaces based on 30 years of interpolated data and is widely used for ecological and environmental studies (Fick and Hijmans, 2017).

2.9. Statistical analysis

All statistical analyses were performed using R version 4.4.1 (R Core Team, 2024). Bar graphs with post hoc Tukey tests were generated using the *ggplot2* package, with Tukey's Honestly Significant Difference (*HSD*) test applied through *TukeyHSD*. Salinity classification was treated as a numerical variable in the ANOVA (1 for oligohaline, 2 for mesohaline, and 3 for polyhaline zones). Scatterplots and regression analyses were conducted using the linear model function (*lm*) in R. We note that principal component analysis and regression models identify statistical associations but cannot establish causal relationships. This study was designed to evaluate spatial patterns of biocapacity and identify key environmental drivers rather than to infer causality. Establishing causal pathways will require longitudinal or experimental datasets, and future work may benefit from approaches such as structural equation modeling (SEM) once such data are available.

3. Results

3.1. Spatial distribution of biocapacity and ecological deficit/reserve on local, national and global level

The spatial distribution of biocapacity (gha/person) and ecological deficit/reserve across the Sundarbans is shown in Fig. 2. Locally, mean biocapacity was highest in the north (1.87 gha/person; 0.64–4.37), moderate in the center (1.22 gha/person; 0.20–2.48), and lowest in the south (0.59 gha/person; 0.04–1.85) (Fig. 2a).

Ecological deficits and reserves exhibited clear spatial gradients (Fig. 2b–d). At the local scale, reserves in the north ranged from 0.17 to 3.90 gha/person (mean 1.40), the center from −0.26 to 2.01 gha/person (mean 0.75), and the south from −0.43 to 1.38 gha/person (mean 0.12). Reserves concentrated in central and northeastern areas, while southern and southwestern zones consistently faced deficits. Similar patterns were observed nationally. Northern reserves ranged from −0.06 to 3.67 gha/person (mean 1.17), central reserves from −0.50 to 1.78 gha/person (mean 0.52), and southern areas showed deeper deficits (−0.66 to 1.15 gha/person; mean −0.11) (Fig. 2c). At the global scale, deficits intensified, particularly in saline southern zones. Southern deficits ranged from −1.56 to 0.25 gha/person (mean −1.01), central from −1.40 to 0.88 gha/person (mean −0.38), while northern reserves varied from −0.96 to 2.77 gha/person (mean 0.27) (Fig. 2d).

These findings highlight a progressive increase in ecological imbalance from local to global scales, with southern regions more vulnerable due to higher salinity and environmental stress.

3.2. Effects of salinity zone on biocapacity and ecological deficit/reserve on local, national and global level

Biocapacity declined significantly across salinity zones, with the oligohaline zone showing the highest mean biocapacity (1.87 ± 0.16 gha/person), followed by mesohaline (1.13 ± 0.17) and polyhaline (0.48 ± 0.10) zones ($R^2 = 0.35$, $p < 0.001$; Fig. 3a). Post hoc Tukey tests confirmed significant differences among all zones.

Similarly, local ecological reserves decreased from oligohaline (1.40 ± 0.16 gha/person) to mesohaline (0.66 ± 0.17) and polyhaline (0.02 ± 0.10) zones relative to the local footprint ($R^2 = 0.32$, $p < 0.001$; Fig. 3b), with all pairwise differences significant. At the national scale, ecological reserves were positive in oligohaline (1.17 ± 0.16) and mesohaline (0.42 ± 0.16) zones but negative in the polyhaline zone (−0.21 ± 0.10 gha/person), indicating a significant downward trend across salinity zones ($R^2 = 0.29$, $p < 0.001$; Fig. 3c), confirmed by Tukey tests. Globally, reserves persisted in the oligohaline zone (0.26 ± 0.16 gha/person), while mesohaline (−0.47 ± 0.16) and polyhaline (−1.11 ± 0.10) zones exhibited escalating deficits (Fig. 3d), with significant differences confirmed at both national and global levels (Fig. 3c and d).

3.3. Multiple driver effects on biocapacity

In the three-dimensional Principal Component Analysis (PCA)

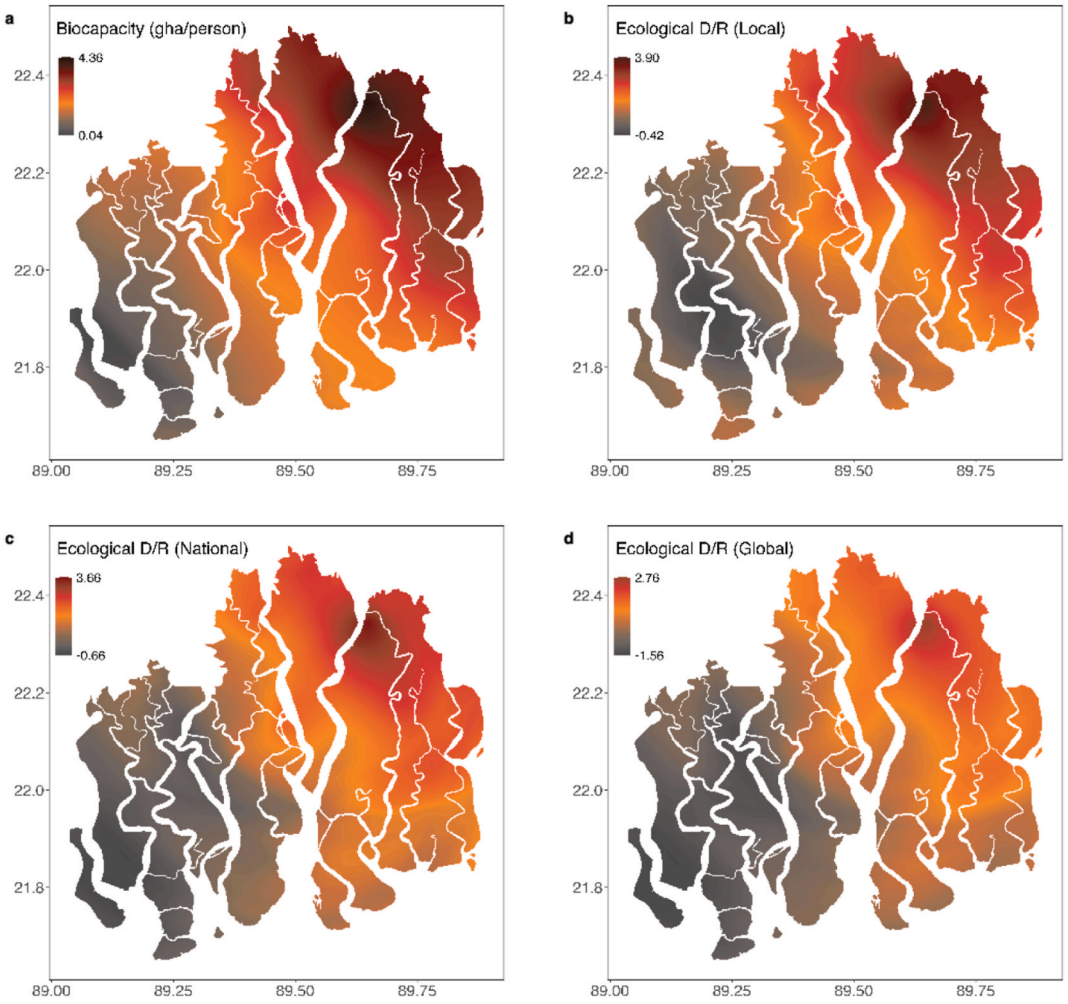

Fig. 2. Spatial distribution of the a) Biocapacity in global hectares per person (gha/person), b) Ecological deficit/reserve (D/R) local level, c) Ecological deficit/reserve national level, and d) Ecological deficit/reserve global level.

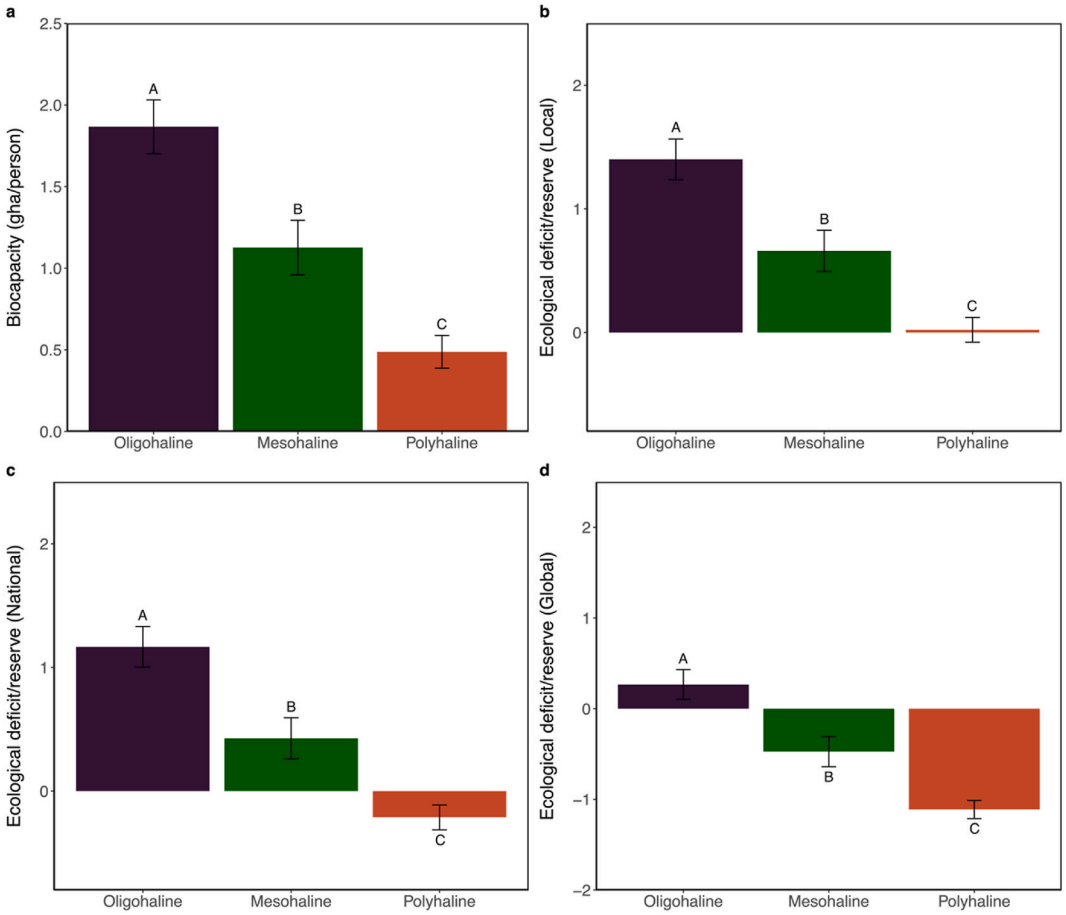

Fig. 3. Bar plot showing different salinity zone vs a) Biocapacity (gha/person), b) Ecological deficit/reserve local level, c) Ecological deficit/reserve national level, and d) Ecological deficit/reserve global level. Statistical significance ($p < 0.05$) among salinity levels was assessed using ANOVA followed by Tukey's HSD test, with different letters indicating significant differences. Different uppercase letters above the bars indicate significant differences between salinity zones within each panel (a–d).

(Fig. 4), 15 drivers explained 51.8 % of the total variation in Sundarban biocapacity (gha·person^{-1}). PC1 accounted for 27.3 % of the variation, while PC2 and PC3 explained 14.6 % and 9.9 %, respectively. Among climatic factors, mean annual temperature ($r = -0.42$) and electrical conductivity ($r = -0.39$), a proxy for soil salinity, exhibited the strongest negative correlations with biocapacity. In contrast, stand structure factors, including mean plot tree height ($r = 0.33$) and average wood density per plot ($r = 0.34$), showed the highest positive correlations with biocapacity (Fig. 4).

3.4. Climatic, environmental and topographic factors

Regression analysis was conducted to evaluate the relationship between biocapacity (gha·person^{-1}) and selected climatic, environmental and topographic factors. A significant negative relation was identified between biocapacity and mean annual temperature (°C) ($R^2 = 0.18$, $p < 0.001$) (Fig. 5a). In contrast, biocapacity was found to be positively related with both annual precipitation (mm) ($R^2 = 0.10$, $p < 0.001$) and elevation (m) ($R^2 = 0.18$, $p < 0.001$) (Fig. 5b and d). No statistically significant relationship was detected between biocapacity and mean wind speed (m·s^{-1}) ($R^2 = 0.04$, $p = 0.22$) (Fig. 5c). ANOVA results further supported these findings. A significant negative association was confirmed between biocapacity and mean annual temperature ($R^2 = 0.16$, $F = 11.23$, $p < 0.001$) (Fig. 5a–Table 1). Biocapacity also showed significant positive relations with annual precipitation ($R^2 = 0.054$, $F = 4.04$, $p < 0.001$) and elevation ($R^2 = 0.12$, $F = 8.76$, $p < 0.001$) (Fig. 5b and d; Table 1). No significant relation was observed between biocapacity and mean wind speed ($R^2 = 0.006$, $F = 1.33$, $p = 0.25$) (Fig. 5c).

3.5. Stand structure and soil properties factor

Biocapacity exhibited significant positive relationship with several stand structure factors. Mean plot tree height (m) was positively associated with biocapacity ($R^2 = 0.11$, $p < 0.05$), indicating that taller trees contribute to higher biocapacity (Fig. 5e–Table 1). Similarly, average wood density (g·cm^{-3}) showed a positive relation with biocapacity ($R^2 = 0.12$, $p < 0.05$) (Fig. 5g). Other structural parameters, including mean plot basal area (cm^2) (Fig. 5f), species abundance (individuals·ha^{-1}) (Fig. 5h), and species richness (species·ha^{-1}) (Fig. 5i), did not show significant relationships with biocapacity ($p > 0.05$). Canopy cover (%) displayed a modest but significant positive association with biocapacity ($R^2 = 0.07$, $p < 0.05$) (Fig. 5j). Among the soil factors, electrical conductivity (mS·cm^{-1}), a proxy for soil salinity, exhibited a strong negative relation with biocapacity ($R^2 = 0.15$, $p < 0.01$) (Fig. 5l–Table 1). Soil pH showed no significant association ($p > 0.05$) (Fig. 5k). Similarly, soil bulk density (g·cm^{-3}) (Fig. 5m), litter organic carbon (t·ha^{-1}) (Fig. 5n), and soil organic carbon (t·ha^{-1}) (Fig. 5o) were not significantly related with biocapacity ($p > 0.05$).

4. Discussion

The spatial distribution and environmental influences on biocapacity and ecological deficit/reserve in the Sundarbans mangrove forest reveal

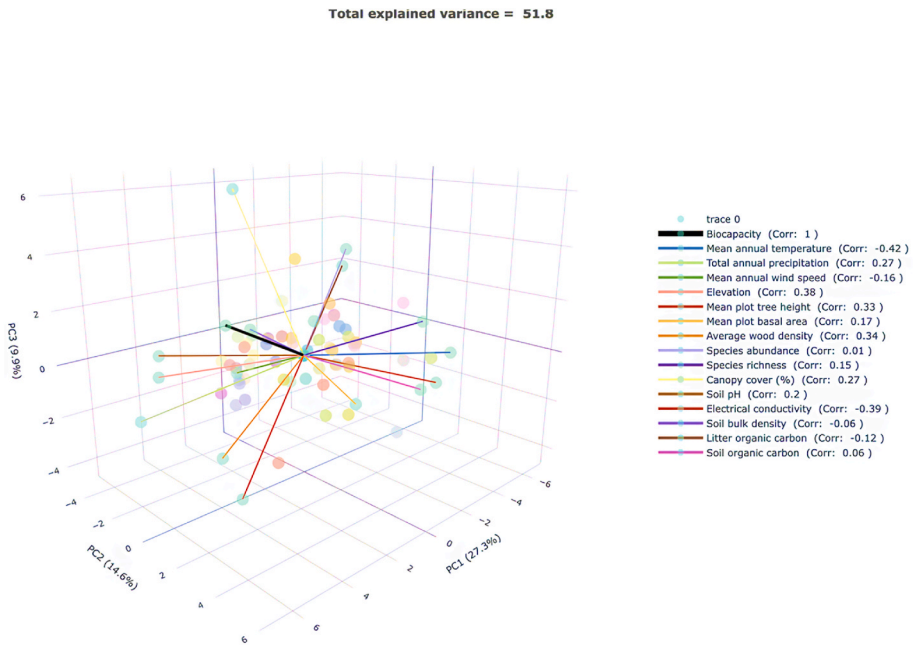

Fig. 4. Three-dimensional principal component analysis (PCA) illustrating the relationship between biocapacity and: a) climatic factors, including mean annual temperature and total annual precipitation; b) environmental and topographic factors, encompassing mean annual wind speed and elevation; c) stand structure characteristics, such as mean plot tree height, mean plot basal area, average wood density, species abundance, species richness, and canopy cover; and d) soil properties, including soil pH, electrical conductivity, soil bulk density, litter organic carbon, and soil organic carbon. Here, corr = correlation values.

intricate patterns of ecological balance influenced by both local and broader-scale factors.

4.1. Spatial distribution and regional variability

The biocapacity distribution across the Sundarbans shows a clear gradient, with higher values (up to 4.36 gha/person) in the northern and central regions and lower values (as low as 0.04 gha/person) in the southern zone. Our results demonstrate a clear gradient in biocapacity, corroborating earlier observations (Kamruzzaman et al., 2017; Tusar et al., 2023), but extend these findings by explicitly linking spatial variability to quantitative measures of ecological deficit/reserve, thereby providing new evidence on how salinity and hydrology shape ecosystem capacity in the Sundarbans. These results reinforce the recognized role of salinity gradients in mangrove productivity (Ahmed et al., 2023; Perri et al., 2023), while our study adds novel quantification of how these gradients influence biocapacity and ecological balance at multiple spatial scales.

In the Sundarbans, these patterns are likely influenced by factors such as salinity and inundation frequency, which regulate resource availability and ecological capacity. The central and northeastern regions, having higher biocapacity, may benefit from more favorable conditions for biotic productivity and ecosystem functioning. Conversely, the southern and southwestern parts face ecological deficits, potentially due to increased salinity, erosion and climatic hazards, which could exacerbate resource scarcity and ecological strain. Similar patterns have been reported in other mangrove systems globally. For example, Ahmed et al. (2022) found declining site quality along increasing salinity gradients in Sundarbans, and Zheng et al. (2023) reported similar findings for China's southern mangroves, where increased salinity and urban pressures reduce ecosystem productivity and biocapacity.

At the national and global scales, the trend persists, with significant ecological deficits observed in the southern and southwestern parts. This is consistent with broader observations of mangrove systems showing how local scale disturbances contribute to larger ecological balances (Duke et al., 2007). The assessed ecological deficits in the southern part at the global scale suggest a critical need for targeted conservation efforts in this region to address the imbalance between resource availability and ecological demand.

4.2. Impact of salinity on biocapacity and ecological balance

Salinity is a key factor influencing the biocapacity and productivity of coastal wetlands, as it significantly regulates carbon allocation and overall ecosystem functioning (Alongi, 1998; Ball, 1988; Perri et al., 2019). Tidal zonation, which affects species distribution and their succession patterns in turn shapes the productivity and ecological balance of these ecosystems and is closely linked to salinity gradients (Perri et al., 2018; Perri and Molini, 2022). Managing coastal wetland ecosystems and maintaining their capacity to support biodiversity and essential ecosystem services requires a comprehensive understanding of the impacts of salinity on these dynamics.

Our analysis of biocapacity and ecological deficit/reserve across different salinity zones highlights the fundamental role of salinity in shaping ecological outcomes. Oligohaline zones, characterized by lower salinity, exhibit the highest biocapacity, indicating that reduced salinity supports higher primary productivity and resource availability in mangrove ecosystems. While previous studies identified salinity as a key limiting factor for biomass and carbon stocks (Adame et al., 2021; Bathmann et al., 2021; Perri et al., 2023; Yoshikai et al., 2022), our work explicitly demonstrates how salinity gradients translate into spatial patterns of biocapacity and ecological deficits in the Sundarbans, providing more direct evidence for ecosystem management. The significant decline in biocapacity from oligohaline to polyhaline zones reflects the detrimental effects of elevated salinity through impeding biotic performance and reducing ecological resilience (Ahmed et al., 2022). At the local level, oligohaline regions demonstrate robust ecological reserves, while polyhaline regions exhibit near-zero ecological balance (Ahmed et al., 2023) reported the higher abundance of small-sized trees in polyhaline zones of the Sundarbans and indicated the impact of salinity on tree growth of mangroves, implying lower productivity of this zone. Nationally, the gradual decline of ecological reserves from oligohaline to polyhaline regions is evident. But globally,

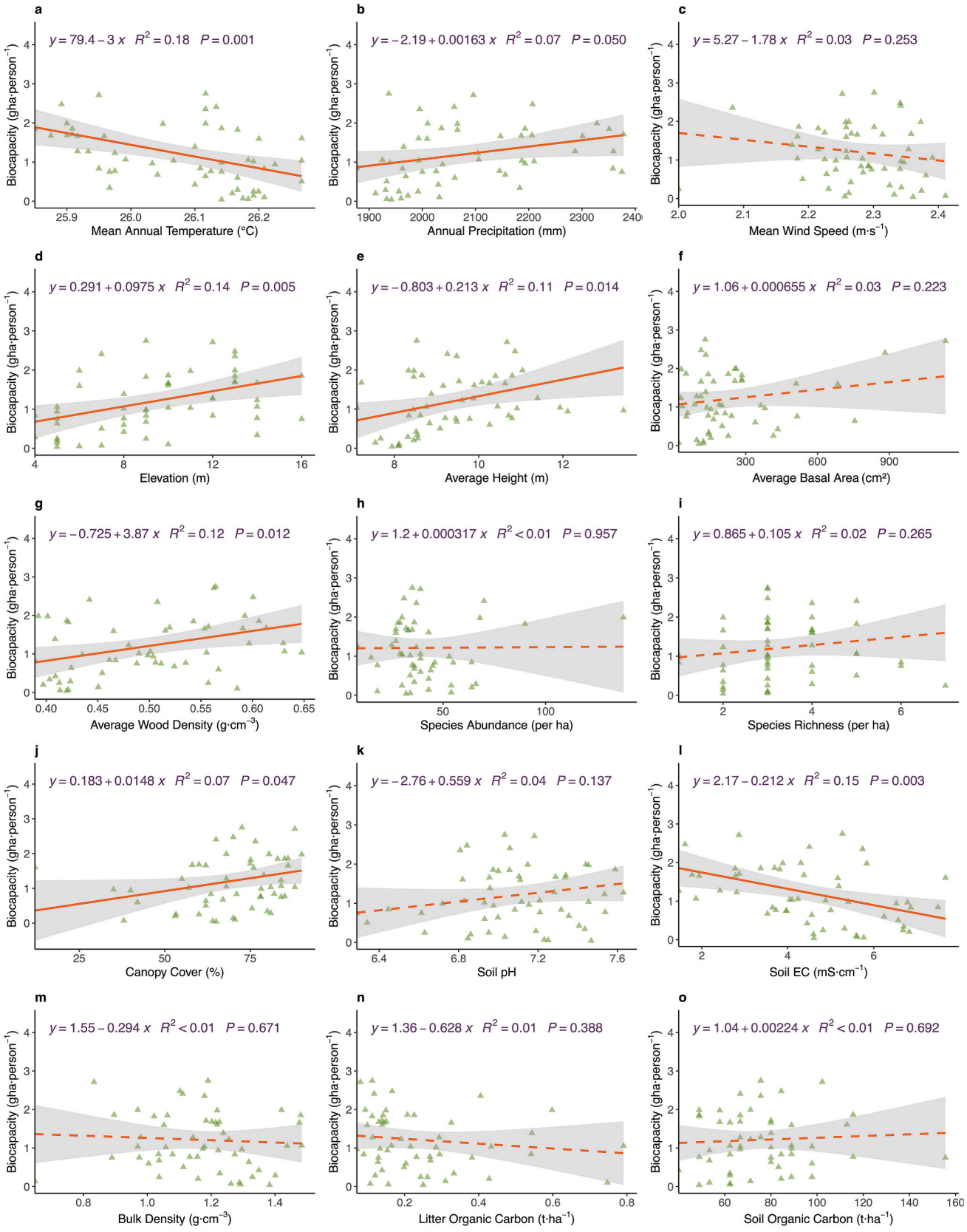

Fig. 5. Scatter plots showing the relationship between biocapacity biomass (gha·person^{-1}) and climatic factors, including **a)** Mean annual temperature (^{o}C) and **b)** Total annual precipitation (mm); environmental and topographic factors, **c)** mean annual wind speed (m·s^{-1}) and **d)** elevation (m); stand structure characteristics, such as **e)** mean plot tree height (m), **f)** mean plot basal area (cm^{2}), **g)** average wood density (g·cm^{-3}), **h)** species abundance (per ha), **i)** species richness (per ha), and **j)** canopy cover (%); and soil properties, including **k)** soil pH, **l)** Electrical conductivity (mS·cm^{-1}), **m)** soil bulk density (g·cm^{-3}), **n)** litter organic carbon (t·ha^{-1}), and **o)** soil organic carbon (t·ha^{-1}).

Table 1
One-way ANOVA of biocapacity (gha per person) associated with environmental factors and climatic variables in the Sundarbans.

Factor class	Factors	F value	p-value
Climate	Mean annual temperature (°C)	11.24	<0.01**
	Total precipitation (mm)	4.042	<0.05*
Environment and Topography	Mean wind speed (m/s)	1.336	0.253
	Elevation (m)	8.762	<0.01**
Stand structure	Mean plot tree height (m)	6.482	<0.05*
	Mean plot basal area (cm^2)	1.52	0.223
	Average wood density ($g{\cdot}cm^{-3}$)	6.79	<0.05*
	Species abundance (per ha)	0.003	0.957
	Species richness (per ha)	1.272	0.265
	Canopy cover (%)	4.144	<0.05*
Soil properties	Soil pH	2.276	0.137
	Electrical conductivity ($mS{\cdot}cm^{-1}$)	9.462	<0.01**
	Soil bulk density ($g{\cdot}cm^{-3}$)	0.183	0.671
	Litter organic carbon ($t{\cdot}ha^{-1}$)	0.759	0.388
	Soil organic carbon ($t{\cdot}ha^{-1}$)	0.159	0.692

polyhaline regions face significant ecological deficits. Though establishing a direct connection between salt stress and ecological balance at the global scale is challenging, our observations provide an explicit impact of salinity on ecological balance across scales.

4.3. Drivers of biocapacity in the Sundarbans

Identifying factors driving the biocapacity of globally important mangroves is crucial for management and conservation. Our study focused on natural factors—climate, environment, stand structure, and soil properties— which explained 51.8 % of the biocapacity variation in the Sundarbans, underscoring their critical role in sustaining ecological and human needs. We acknowledge that 48.2 % of the variation remains unexplained, typical in complex ecosystems due to unmeasured variables, natural variability, and system complexity (Legendre and Legendre, 2012).

Climate, especially temperature and precipitation, were significant drivers of biocapacity. Climatic factors regulate physiological processes, productivity, carbon sequestration, and species distribution (Fu et al., 2017; Mao et al., 2022; Zhou et al., 2016). Temperature limits mangrove range and biodiversity; we found a negative correlation between biocapacity and mean annual temperature, suggesting potential declines under warming scenarios (Duke et al., 1998; Osland et al., 2016; Rivera-Monroy et al., 2017). Conversely, biocapacity positively correlated with precipitation, supporting mangrove expansion and productivity via enhanced sediment and nutrient delivery through river discharge (Donato et al., 2011; Eslami-Andargoli et al., 2009; Rasquinha and Mishra, 2021; Sanders et al., 2016). These dynamics emphasize the vulnerability of this mangrove ecosystem in the context of future climate change.

Soil properties were selected based on their ecological relevance and prior studies identifying soil chemistry as a key driver in mangroves (Alongi, 2021). We included pH, electrical conductivity (EC), organic carbon, nitrogen, and phosphorus to represent soil chemical conditions affecting plant growth and carbon storage. EC, a proxy for salinity, was the only significant soil correlate, reflecting salinity's dominant role in limiting mangrove productivity (Wang et al., 2018; Ahmed et al., 2022), while other soil variables showed weaker or non-significant relationships, consistent with previous findings.

Sundarbans' low elevation influences topography, tidal inundation, soil salinity, and species survival, making it vulnerable to sea-level rise, which will likely reduce biocapacity as inundation regimes shift (Kumari et al., 2020a). Elevation also affects soil pH and nitrogen, both crucial for mangrove growth and carbon sequestration (Huang et al., 2023; Meng et al., 2022). Stand structure also impacts biocapacity; positive relationships between tree height, wood density, and biocapacity indicate taller, denser trees enhance ecosystem capacity. This supports conserving and restoring healthy forest structure to sustain the Sundarbans productivity.

Recognizing climate, salinity, and stand structure as key drivers, conservation strategies should integrate dynamic, data-driven management. This study supports ecosystem-based adaptation (EbA), combining predictive modeling with stakeholder engagement to build resilience. Findings from the Sundarbans provide a foundation for adaptive policies applicable to mangrove systems globally, promoting scalable climate mitigation and biodiversity conservation. Future research should employ advanced modeling techniques, such as machine learning, to further unravel complex ecological interactions with climatic and anthropogenic factors.

4.4. Global implications of the findings

Our study offers a comprehensive evaluation of the drivers that shape biocapacity in Sundarbans, the world's largest mangrove forest, by providing critical insights into how variables such as climate, salinity and stand structure influence this globally vital ecosystem. Mangrove forests globally are recognized for their multifaceted ecological functions that include carbon sequestration, shoreline stabilization, and support for diverse marine and terrestrial species (Kumari et al., 2020b; Lee et al., 2014). However, our study findings highlight how the Sundarbans facing increasing challenges from climate change, affecting its ability to sustain ecological balance.

Much like terrestrial ecosystem conservation strategies that must consider both local contexts and broader ecological dynamics, mangrove conservation requires an integrated approach. Exploration of biocapacity drivers in our study uncovers how the local factors mirror global environmental patterns. For example, the negative impact of temperature aligns with broader climate change trends, suggesting that rising global temperatures may diminish the ecological capacity of mangroves worldwide. Conversely, the positive relationship of structural factors like tree height, wood density reinforces the global importance of structurally diverse forests in maintaining ecosystem functions. Seasonal and interannual changes in water temperature, sea level, and salinity are fundamental drivers of mangrove distribution, productivity, and resilience. These hydrological factors interact with climate and geomorphology to shape resource availability, species turnover, and stress responses. Rising sea levels alter inundation, sediment supply, and nutrient delivery, while fluctuations in water temperature affect physiology and reproduction, with lasting impacts on stability (Fu et al., 2025; Yao et al., 2025). Recognizing these controls provides a fuller understanding of ecological balance and emphasizes the need to integrate freshwater inflow management into conservation policy.

The observed ecological deficits in the southern and southwestern regions of the Sundarbans align with global patterns of mangrove under ecological stress, underscoring the need for comprehensive conservation strategies that address both local and global environmental challenges. The observed ecological reserves are located very close to local communities and are more vulnerable to anthropogenic disturbances suggesting planned protection and conservation. Failing to address local needs could undermine long-term conservation efforts.

Future research on global mangrove biocapacity could benefit from incorporating additional environmental factors such as seasonal water temperature and hydrometeorological dynamics, which are known to influence short-term physiological responses.

Finally, our study provides a framework for assessing the impacts of environmental changes on large-scale mangrove ecosystems and suggests that future research should continue to explore these dynamics to inform conservation strategies and enhance ecosystem resilience in the face of ongoing environmental changes.

5. Conclusion

This study provides a comprehensive assessment of the biocapacity and ecological balance of the Sundarbans, highlighting its spatial variations at local, national, and global scales. It reveals that northern and central parts have higher biocapacity compared to the southern part, which struggles with ecological deficits. Unlike previous studies that focused solely on carbon storage or species diversity, this study uniquely links ecological provisioning directly with human needs, quantitatively coupling biological carrying capacity with salinity gradients and climatic factors. Salinity emerges as a key factor of biocapacity variation and ecological balance revealing the complex interaction between environmental factors and resource availability. Climatic variables, particularly mean annual temperature and annual precipitation, significantly affect biocapacity, while wind speed has negligible effects. These findings enhance our understanding of the Sundarbans' ecological dynamics and emphasize the need for integrated conservation strategies. Future research should focus on integrating these findings with climate change models to develop predictive tools for policymakers in environmental management and coastal conservation planning. Globally, this study contributes valuable insights to inform broader conservation efforts for mangrove ecosystems, highlighting the Sundarbans as a model system for assessing the coupling of ecological capacity, environmental gradients, and human demand, thereby underscoring its innovative contribution to mangrove research.

CRediT authorship contribution statement

Md Rezaul Karim: Writing – original draft, Software, Methodology, Investigation, Formal analysis, Data curation, Conceptualization. **Md Shamim Reza Saimun:** Writing – original draft, Data curation, Conceptualization. **Hossain Mahmud Sammi:** Writing – original draft, Investigation. **Ariful Khan:** Writing – original draft, Investigation. **Md Sahinur Islam Fahim:** Writing – review & editing. **Fahmida Sultana:** Writing – review & editing. **Sanjeev K. Srivastava:** Writing – review & editing, Funding acquisition. **Pallab Mozumder:** Writing – review & editing. **Daniel Friess:** Writing – review & editing. **Sharif A. Mukul:** Writing – review & editing, Funding acquisition, Conceptualization. **Mohammed A.S. Arfin-Khan:** Writing – review & editing, Supervision, Methodology, Funding acquisition, Conceptualization.

Declaration of competing interest

The authors declare that they have no known competing financial interests or personal relationships that could have appeared to influence the work reported in this paper.

Acknowledgements

The authors would like to acknowledge the funding support received from various organizations. Sanjeev K. Srivastava was supported by a grant from the Asia Pacific Network for Global Change Research, Japan (Project code: CRRP2020-08MY-Srivastava); Sharif A. Mukul was supported by a grant from the National Geographic Society, USA (Grant reference number: NGS-78528R-22) and the British Ecological Society, UK (Grant reference number: BES LRB20-1006); and Mohammed A. S. Arfin-Khan was supported by three grants from the SUST Research Center, Bangladesh (Grant reference numbers: FES/2021/2/04, FES/2022/1/09, and FES/2023/2/01). The authors also acknowledge the valuable feedback provided by three anonymous reviewers, which substantially improved the quality of the manuscript.

Appendix A. Supplementary data

Supplementary data to this article can be found online at https://doi.org/10.1016/j.jenvman.2025.127815.

Data availability

Data will be made available on request.

References

Adame, M.F., Reef, R., Santini, N.S., Najera, E., Turschwell, M.P., Hayes, M.A., Masque, P., Lovelock, C.E., 2021. Mangroves in arid regions: ecology, threats, and opportunities. Estuar. Coast Shelf Sci. 248, 106796.

Ahmed, S., Sarker, S.K., Friess, D.A., Kamruzzaman, M., Jacobs, M., Islam, M.A., Alam, M.A., Suvo, M.J., Sani, M.N.H., Dey, T., 2022. Salinity reduces site quality and mangrove forest functions. From monitoring to understanding. Sci. Total Environ. 853, 158662.

Ahmed, S., Sarker, S.K., Friess, D.A., Kamruzzaman, M., Jacobs, M., Sillanpää, M., Naabeh, C.S.S., Pretzsch, H., 2023. Mangrove tree growth is size-dependent across a large-scale salinity gradient. For. Ecol. Manag. 537, 120954.

Ahmed, S.K., Rahman, MdS., 2023. Protecting the Bengal tiger in the Sundarbans, Bangladesh: conservation measures reconsidered. Int. J. Environ. Stud. 80, 1283–1298. https://doi.org/10.1080/00207233.2023.2224667.

Akber, MdA., Patwary, M.M., Islam, MdA., Rahman, M.R., 2018. Storm protection service of the Sundarbans mangrove forest, Bangladesh. Nat. Hazards 94, 405–418. https://doi.org/10.1007/s11069-018-3395-8.

Alongi, D.M., 2021. Macro- and micronutrient cycling and crucial linkages to geochemical processes in mangrove ecosystems. J. Mar. Sci. Eng. 9. https://doi.org/10.3390/jmse9050456.

Alongi, D.M., 1998. Coastal Ecosystem Processes. CRC press.

Angelsen, A., Martius, C., De Sy, V., Duchelle, A.E., Larson, A.M., Pham, T.T., 2018. Transforming REDD+: Lessons and New Directions. CIFOR.

Aziz, A., Paul, A.R., 2015. Bangladesh Sundarbans: present status of the environment and biota. Diversity 7, 242–269.

Ball, M.C., 1988. Ecophysiology of mangroves. Trees (Berl.) 2, 129–142.

Banerjee, K., Gatti, R.C., Mitra, A., 2017. Climate change-induced salinity variation impacts on a stenoecious mangrove species in the Indian Sundarbans. Ambio 46, 492–499. https://doi.org/10.1007/s13280-016-0839-9.

Barr, J.G., Engel, V., Fuentes, J.D., Fuller, D.O., Kwon, H., 2013. Modeling light use efficiency in a subtropical mangrove forest equipped with CO_2 eddy covariance. Biogeosciences 10, 2145–2158. https://doi.org/10.5194/bg-10-2145-2013.

Bathmann, J., Peters, R., Reef, R., Berger, U., Walther, M., Lovelock, C.E., 2021. Modelling mangrove forest structure and species composition over tidal inundation gradients: the feedback between plant water use and porewater salinity in an arid mangrove ecosystem. Agric. For. Meteorol. 308, 108547.

BBS, 2022. Population and Housing Census 2022, Preliminary Report. Bangladesh Bureau of Statistics, Ministry of Planning, GoB, Dhaka, Bangladesh.

Bera, B., Bhattacharjee, S., Sengupta, N., Shit, P.K., Adhikary, P.P., Sengupta, D., Saha, S., 2022. Significant reduction of carbon stocks and changes of ecosystem service valuation of Indian Sundarban. Sci. Rep. 12, 7809. https://doi.org/10.1038/s41598-022-11716-5.

BFD, 2017. Natural Mangrove Forest (Sundarbans).

Borrell, A., Tornero, V., Bhattacharjee, D., Aguilar, A., 2016. Trace element accumulation and trophic relationships in aquatic organisms of the Sundarbans mangrove ecosystem (Bangladesh). Sci. Total Environ. 545–546, 414–423. https://doi.org/10.1016/j.scitotenv.2015.12.046.

Bunting, P., Rosenqvist, A., Hilarides, L., Lucas, R.M., Thomas, N., Tadono, T., Worthington, T.A., Spalding, M., Murray, N.J., Rebelo, L.-M., 2022. Global mangrove extent change 1996–2020: Global mangrove watch version 3.0. Remote Sens. 14. https://doi.org/10.3390/rs14153657.

Chave, J., Réjou-Méchain, M., Búrquez, A., Chidumayo, E., Colgan, M.S., Delitti, W.B.C., Duque, A., Eid, T., Fearnside, P.M., Goodman, R.C., Henry, M., Martínez-Yrízar, A., Mugasha, W.A., Muller-Landau, H.C., Mencuccini, M., Nelson, B.W., Ngomanda, A., Nogueira, E.M., Ortiz-Malavassi, E., Pélissier, R., Ploton, P., Ryan, C.M., Saldarriaga, J.G., Vieilledent, G., 2014. Improved allometric models to estimate the aboveground biomass of tropical trees. Glob. Change Biol. 20, 3177–3190. https://doi.org/10.1111/gcb.12629.

Chowdhury, M.S., Hafsa, B., 2022. Multi-decadal land cover change analysis over Sundarbans mangrove forest of Bangladesh: a GIS and remote sensing based approach. Glob. Ecol. Conserv. 37, e02151.

Chowdhury, M.Q., Sarker, S.K., Marma, M., Rahman, M.S., Datta, A., 2024. Climate and salinity together control above ground carbon accumulation in the Sundarbans mangrove ecosystem. Ocean Coast. Manag. 255, 107242. https://doi.org/10.1016/j.ocecoaman.2024.107242.

Donato, D.C., Kauffman, J.B., Murdiyarso, D., Kurnianto, S., Stidham, M., Kanninen, M., 2011. Mangroves among the most carbon-rich forests in the tropics. Nat. Geosci. https://doi.org/10.1038/ngeo1123.

Duke, N.C., Ball, M., Ellison, J., 1998. Factors influencing biodiversity and distributional gradients in mangroves. Global Ecol. Biogeogr. Lett. 7, 27–47.

Duke, N.C., Meynecke, J.-O., Dittmann, S., Ellison, A.M., Anger, K., Berger, U., Cannicci, S., Diele, K., Ewel, K.C., Field, C.D., 2007. A world without mangroves? Science 317, 41–42.

Dworatzek, P., Miller, E., Lo, K., Howarth, E., Kazubowski-Houston, S.. National Ecological Footprint and Biocapacity Accounts, 2024 Edition (Version 1.0) [dataset]. York University Ecological Footprint Initiative, Footprint Data Foundation, in partnership with Global Footprint Network. https://footprint.info.yorku.ca/data/.

Eslami-Andargoli, L., Dale, P.E.R., Sipe, N., Chaseling, J., 2009. Mangrove expansion and rainfall patterns in Moreton Bay, southeast Queensland, Australia. Estuar. Coast Shelf Sci. 85, 292–298.
FAO, 2020. Global forest resources assessment 2020: main report (No. 9789251329740). https://doi.org/10.4324/9781315184487-1.
FDF, 2023. Footprint Data Foundation, York University Ecological Footprint Initiative, and Global Footprint Network: National Footprint and Biocapacity Accounts, 2023 edition [WWW Document]. Footpr. Data Found. URL. https://data.footprintnetwork.org. 9.3.24).
Fick, S.E., Hijmans, R.J., 2017. WorldClim 2: new 1-km spatial resolution climate surfaces for global land areas. Int. J. Climatol. 37, 4302–4315. https://doi.org/10.1002/joc.5086.
Flores, O., Coomes, D.A., 2011. Estimating the wood density of species for carbon stock assessments. Methods Ecol. Evol. 2, 214–220. https://doi.org/10.1111/j.2041-210X.2010.00068.x.
Friess, D.A., Adame, M.F., Adams, J.B., Lovelock, C.E., 2022. Mangrove forests under climate change in a 2°C world. WIREs Clim. Change 13, e792. https://doi.org/10.1002/wcc.792.
Fu, B., Yuan, B., Yao, H., Sun, W., Jia, M., Yao, Z., Wang, Y., 2025. Spatio-temporal dynamics of invasive Spartina Alterniflora and its functional traits' responding to hydro-meteorology. Earths Future 13, e2024EF005421. https://doi.org/10.1029/2024EF005421.
Fu, Z., Stoy, P.C., Luo, Y., Chen, J., Sun, J., Montagnani, L., Wohlfahrt, G., Rahman, A.F., Rambal, S., Bernhofer, C., Wang, J., Shirkey, G., Niu, S., 2017. Climate controls over the net carbon uptake period and amplitude of net ecosystem production in temperate and boreal ecosystems. Agric. For. Meteorol. 243, 9–18. https://doi.org/10.1016/j.agrformet.2017.05.009.
Gilang Qur'ani, C., Lee, B., Sasmito, S.D., Maulana, A.M., Seol, M., Wiradana, P.A., Leksono, B., Watiniasih, N.L., Baral, H., 2024. Natural and anthropogenic impacts on mangrove carbon dynamics: a systematic review protocol. For. Sci. Technol. 20, 1–7. https://doi.org/10.1080/21580103.2023.2272705.
GoB, 2019. Tree and Forest Resources of Bangladesh: Report on the Bangladesh Forest Inventory. Forest Department, Ministry of Environment, Forest and Climate Change, Government of the People's Republic of Bangladesh, Dhaka, Bangladesh.
Gopal, B., Chauhan, M., 2018. The transboundary Sundarbans mangroves (India and Bangladesh). In: Finlayson, C.M., Milton, G.R., Prentice, R.C., Davidson, N.C. (Eds.), The Wetland Book: II: Distribution, Description, and Conservation. Springer, Netherlands, Dordrecht, pp. 1733–1742. https://doi.org/10.1007/978-94-007-4001-3_26.
Gouvêa, L.P., Serrão, E.A., Cavanaugh, K., Gurgel, C.F.D., Horta, P.A., Assis, J., 2022. Global impacts of projected climate changes on the extent and aboveground biomass of mangrove forests. Divers. Distrib. 28, 2349–2360. https://doi.org/10.1111/ddi.13631.
Guild, R., Wang, X., Quijón, P.A., 2025. Climate change impacts on coastal ecosystems. Environ. Res. Clim. 3, 042006. https://doi.org/10.1088/2752-5295/ad9f90.
Hale, R.P., Wilson, C.A., Bomer, E.J., 2019. Seasonal variability of forces controlling sedimentation in the Sundarbans national forest, Bangladesh. Front. Earth Sci. 7, 211, 211.
Howe, J., Merchant, S., Hernández, W.J., Pessutti, J., Groffman, P., 2025. Assessing mangrove canopy height and health changes in Puerto Rico post-Hurricane Maria using remote-sensing techniques. Ecosphere 16, e70226. https://doi.org/10.1002/ecs2.70226.
Huang, X., Feng, J., Yang, Q., Chen, L., Zhang, J., Yang, B., Tang, X., Yu, C., Ling, J., Dong, J., 2023. High site elevation enhanced nitrogen fixation and the stability of diazotrophic community in planted Sonneratia apetala mangrove sediments. Appl. Soil Ecol. 191, 105059. https://doi.org/10.1016/j.apsoil.2023.105059, 105059.
Iqbal, MdH., 2020. Valuing ecosystem services of Sundarbans mangrove forest: approach of choice experiment. Glob. Ecol. Conserv. 24, e01273. https://doi.org/10.1016/j.gecco.2020.e01273.
Islam, M.M., Sunny, A.R., Hossain, M.M., Friess, D.A., 2018. Drivers of mangrove ecosystem service change in the Sundarbans of Bangladesh. Singapore J. Trop. Geogr. 39, 244–265. https://doi.org/10.1111/sjtg.12241.
Islam, S., Rahman, M., Chakma, S., 2014. Plant diversity and forest structure of the three protected areas (wildlife sanctuaries) of Bangladesh Sundarbans: current status and management strategies. In: Faridah-Hanum, I., Latiff, A., Hakeem, K.R., Ozturk, M. (Eds.), Mangrove Ecosystems of Asia: Status, Challenges and Management Strategies. Springer, New York, New York, NY, pp. 127–152. https://doi.org/10.1007/978-1-4614-8582-7_7.
Jia, M., Wang, Z., Mao, D., Ren, C., Song, K., Zhao, C., Wang, C., Xiao, X., Wang, Y., 2023. Mapping global distribution of mangrove forests at 10-m resolution. Sci. Bull. 68, 1306–1316. https://doi.org/10.1016/j.scib.2023.05.004.
Kamruzzaman, Md, Ahmed, S., Osawa, A., 2017. Biomass and net primary productivity of mangrove communities along the oligohaline zone of Sundarbans, Bangladesh. For. Ecosyst. 4, 16. https://doi.org/10.1186/s40663-017-0104-0.
Kumar, S., Chatterjee, U., David Raj, A., 2022. In: Chatterjee, U., Akanwa, A.O., Kumar, S., Singh, S.K., Dutta Roy, A. (Eds.), Ecological Footprints in Changing Climate: an Overview BT - Ecological Footprints of Climate Change: Adaptive Approaches and Sustainability. Springer International Publishing, Cham, pp. 3–30. https://doi.org/10.1007/978-3-031-15501-7_1.
Kumari, P., Singh, J.K., Pathak, B., 2020a. In: Patra, J.K., Mishra, R.R., Thatoi, H.B.T.-B. U., of, M.R. (Eds.), Chapter 1 - Potential Contribution of Multifunctional Mangrove Resources and its Conservation. Academic Press, pp. 1–26. https://doi.org/10.1016/B978-0-12-819532-1.00001-9.
Kumari, P., Singh, J.K., Pathak, B., 2020b. In: Patra, J.K., Mishra, R.R., Thatoi, H.B.T.-B. U., of, M.R. (Eds.), Chapter 1 - Potential Contribution of Multifunctional Mangrove Resources and its Conservation. Academic Press, pp. 1–26. https://doi.org/10.1016/B978-0-12-819532-1.00001-9.
Lee, S.Y., Primavera, J.H., Dahdouh-Guebas, F., McKee, K., Bosire, J.O., Cannicci, S., Diele, K., Fromard, F., Koedam, N., Marchand, C., Mendelssohn, I., Mukherjee, N., Record, S., 2014. Ecological role and services of tropical mangrove ecosystems: a reassessment. Global Ecol. Biogeogr. 23, 726–743. https://doi.org/10.1111/geb.12155.
Legendre, P., Legendre, L., 2012. Chapter 1 - Complex ecological data sets. In: Legendre, P., Legendre, L. (Eds.), Developments in Environmental Modelling. Elsevier, pp. 1–57. https://doi.org/10.1016/B978-0-444-53868-0.50001-0.
Lo, K., Miller, E., Dworatzek, P., Basnet, N., Silva, J., Van Berkum, J.L., Halldórsdóttir, R. B., Dyck, M.D.R., 2025. National Ecological Footprint and Biocapacity Accounts, 2025 Edition.
Mahmood, H., Ahmed, M., Islam, T., Uddin, M.Z., Ahmed, Z.U., Saha, C., 2021. Paradigm shift in the management of the Sundarbans mangrove forest of Bangladesh: issues and challenges. Trees For. People 5, 100094, 100094.
Maina, J.M., Bosire, J.O., Kairo, J.G., Bandeira, S.O., Mangora, M.M., Macamo, C., Ralison, H., Majambo, G., 2021. Identifying global and local drivers of change in mangrove cover and the implications for management. Global Ecol. Biogeogr. 30, 2057–2069. https://doi.org/10.1111/geb.13368.
Mandal, M.S.H., Hosaka, T., 2020. Assessing cyclone disturbances (1988–2016) in the Sundarbans mangrove forests using landsat and google Earth engine. Nat. Hazards 102, 133–150. https://doi.org/10.1007/s11069-020-03914-z.
Mao, F., Du, H., Zhou, G., Zheng, J., Li, X., Xu, Y., Huang, Z., Yin, S., 2022. Simulated net ecosystem productivity of subtropical forests and its response to climate change in Zhejiang Province, China. Sci. Total Environ. 838, 155993. https://doi.org/10.1016/j.scitotenv.2022.155993, 155993.
Meng, Y., Gou, R., Bai, J., Moreno-Mateos, D., Davis, C.C., Wan, L., Song, S., Zhang, H., Zhu, X., Lin, G., 2022. Spatial patterns and driving factors of carbon stocks in mangrove forests on Hainan Island, China. Global Ecol. Biogeogr. 31, 1692–1706.
Mishra, M., Acharyya, T., Santos, C.A.G., Silva, R.M. da, Kar, D., Mustafa Kamal, A.H., Raulo, S., 2021. Geo-ecological impact assessment of severe cyclonic storm Amphan on Sundarban mangrove forest using geospatial technology. Estuar. Coast Shelf Sci. 260, 107486. https://doi.org/10.1016/j.ecss.2021.107486.
Monfreda, C., Wackernagel, M., Deumling, D., 2004. Establishing national natural capital accounts based on detailed ecological footprint and biological capacity assessments. Land Use Sustain. Indic. 21, 231–246. https://doi.org/10.1016/j.landusepol.2003.10.009.
Niccolucci, V., Tiezzi, E., Pulselli, F.M., Capineri, C., 2012. Biocapacity vs ecological footprint of world regions: a geopolitical interpretation. State Art Ecol. Footpr. Theory Appl. 16, 23–30. https://doi.org/10.1016/j.ecolind.2011.09.002.
Oliver, M.A., Webster, R., 2014. A tutorial guide to geostatistics: computing and modelling variograms and kriging. Catena 113, 56–69. https://doi.org/10.1016/j.catena.2013.09.006.
Osland, M.J., Enwright, N.M., Day, R.H., Gabler, C.A., Stagg, C.L., Grace, J.B., 2016. Beyond just sea-level rise: considering macroclimatic drivers within coastal wetland vulnerability assessments to climate change. Glob. Change Biol. 22, 1–11.
Panda, M., Lele, N., Murthy, T.V.R., Samal, R.N., Pattnaik, A.K., Sahu, S.C., 2024. Assessment of mangrove stand biomass in relation to forest structural attributes in Bhitarkanika national park, India. Vegetos 37, 950–960. https://doi.org/10.1007/s42535-023-00630-4.
Patel, R., Mukherjee, S., Sahu, B., Dash, B., Jaison, M., Avinash, K., Singh, P., 2024. Sustainable forest management (SFM) for C footprint and climate change mitigation. In: Agroforestry to Combat Global Challenges: Current Prospects and Future Challenges. Springer, pp. 203–217.
Payo, A., Mukhopadhyay, A., Hazra, S., Ghosh, T., Ghosh, S., Brown, S., Nicholls, R.J., Bricheno, L., Wolf, J., Kay, S., Lázár, A.N., Haque, A., 2016. Projected changes in area of the Sundarban mangrove forest in Bangladesh due to SLR by 2100. Clim. Change 139, 279–291. https://doi.org/10.1007/s10584-016-1769-z.
Pearson, T.R.H., Brown, S.L., Birdsey, R.A., 2007. Measurement Guidelines for the Sequestration of Forest Carbon, 18. U.S. Department of Agriculture, Forest Service, Northern Research Station. https://doi.org/10.2737/nrs-gtr-18.
Perri, S., Detto, M., Porporato, A., Molini, A., 2023. Salinity-induced limits to mangrove canopy height. Global Ecol. Biogeogr. 32, 1561–1574.
Perri, S., Katul, G.G., Molini, A., 2019. Xylem–phloem hydraulic coupling explains multiple osmoregulatory responses to salt stress. New Phytol. 224, 644–662.
Perri, S., Molini, A., 2022. Declining Hydrologic Function of Coastal Wetlands in Response to Saltwater Intrusion. ArXiv Prepr. ArXiv220800903.
Perri, S., Suweis, S., Entekhabi, D., Molini, A., 2018. Vegetation controls on dryland salinity. Geophys. Res. Lett. 45, 11–669.
R Core Team, 2024. R: a Language and Environment for Statistical Computing.
Rasquinha, D.N., Mishra, D.R., 2021. Tropical cyclones shape mangrove productivity gradients in the Indian subcontinent. Sci. Rep. 11, 17355. https://doi.org/10.1038/s41598-021-96752-3, 17355.
Rivera-Monroy, V.H., Osland, M.J., Day, J.W., Ray, S., Rovai, A., Day, R.H., Mukherjee, J., 2017. In: Rivera-Monroy, V.H., Lee, S.Y., Kristensen, E., Twilley, R.R. (Eds.), Advancing Mangrove Macroecology BT - Mangrove Ecosystems: a Global Biogeographic Perspective: Structure, Function, and Services. Springer International Publishing, Cham, pp. 347–381. https://doi.org/10.1007/978-3-319-62206-4_11.
Roy, S.S., Ghosh, T., Hewavithana, D.K., 2024. Transformation of coastal wetlands in the Sundarban Delta (1999–2020). Environ. Monit. Assess. 196, 758. https://doi.org/10.1007/s10661-024-12901-x, 758.
Sahavacharin, A., Sompongchaiyakul, P., Thaitakoo, D., 2022. The effects of land-based change on coastal ecosystems. Landsc. Ecol. Eng. 18, 351–366. https://doi.org/10.1007/s11355-022-00505-x.

Sanders, C.J., Maher, D.T., Tait, D.R., Williams, D., Holloway, C., Sippo, J.Z., Santos, I.R., 2016. Are global mangrove carbon stocks driven by rainfall? J. Geophys. Res. Biogeosciences 121, 2600–2609.

Sarker, S., Hussain, F.A., Assaduzzaman, M., Failler, P., 2019. Blue economy and climate change: bangladesh perspective. J. Ocean Coast. Econ. 6, 6, 6.

Sarkodie, S.A., 2021. Environmental performance, biocapacity, carbon & ecological footprint of nations: drivers, trends and mitigation options. Sci. Total Environ. 751, 141912. https://doi.org/10.1016/j.scitotenv.2020.141912.

Sen, H.S., Ghorai, D., 2019. The sundarbans: a flight into the wilderness. In: Sen, H.S. (Ed.), The Sundarbans: a Disaster-Prone Eco-Region: Increasing Livelihood Security. Springer International Publishing, Cham, pp. 3–28. https://doi.org/10.1007/978-3-030-00680-8_1.

Sharma, S., Ray, R., Martius, C., Murdiyarso, D., 2023. Carbon stocks and fluxes in Asia-Pacific mangroves: current knowledge and gaps. Environ. Res. Lett. 18, 44002. https://doi.org/10.1088/1748-9326/acbf6c.

Siddique, N.A., 2001. Mangrove Forestry in Bangladesh. Institute of Forestry & Environmental Sciences, University of Chittagong, Chittagong, Bangladesh.

Tasneem, S., Ahsan, MdN., 2024. A bibliometric analysis on mangrove ecosystem services: past trends and emerging interests. Ocean Coast Manag. 256, 107276. https://doi.org/10.1016/j.ocecoaman.2024.107276.

Tusar, M.K., Hasan, M.A., Sultana, N., 2023. Sundarbans mangrove mapping and above ground biomass estimation using earth observation techniques. J. Sustain. Environ. Manag. 2, 126–132.

Twilley, R.R., Castañeda-Moya, E., Rivera-Monroy, V.H., Rovai, A., 2017. In: Rivera-Monroy, V.H., Lee, S.Y., Kristensen, E., Twilley, R.R. (Eds.), Productivity and Carbon Dynamics in Mangrove Wetlands BT - Mangrove Ecosystems: a Global Biogeographic Perspective: Structure, Function, and Services. Springer International Publishing, Cham, pp. 113–162. https://doi.org/10.1007/978-3-319-62206-4_5.

Wackernagel, M., Rees, W., 1996. Our ecological footprint: reducing human impact on the earth. New Society Publishers.

Wang, H., Gilbert, J.A., Zhu, Y., Yang, X., 2018. Salinity is a key factor driving the nitrogen cycling in the mangrove sediment. Sci. Total Environ. 631–632, 1342–1349. https://doi.org/10.1016/j.scitotenv.2018.03.102.

Yao, H., Fu, B., Sun, W., Zhou, Y., Wang, Y., Jiang, W., He, H., Chen, Z., Song, Y., 2025. Quantifying key indicators of essential biodiversity variables for mangrove species in response to hydro-meteorological factors. Int. J. Appl. Earth Obs. Geoinformation 139, 104535. https://doi.org/10.1016/j.jag.2025.104535.

Yoshikai, M., Nakamura, T., Suwa, R., Sharma, S., Rollon, R., Yasuoka, J., Egawa, R., Nadaoka, K., 2022. Predicting mangrove forest dynamics across a soil salinity gradient using an individual-based vegetation model linked with plant hydraulics. Biogeosciences 19, 1813–1832.

Zaman, K., 2022. Environmental cost of deforestation in Brazil's Amazon rainforest: controlling biocapacity deficit and renewable wastes for conserving forest resources. For. Ecol. Manag. 504, 119854. https://doi.org/10.1016/j.foreco.2021.119854.

Zheng, Y., Takeuchi, W., 2022. Estimating mangrove forest gross primary production by quantifying environmental stressors in the coastal area. Sci. Rep. 12, 2238. https://doi.org/10.1038/s41598-022-06231-6.

Zheng, Y., Takeuchi, W., Jiang, Q., 2023. Assessing mangrove conservation in China by integrating mangrove ecosystem into ecological footprint accounting. Ocean Coast Manag. 242, 106728. https://doi.org/10.1016/j.ocecoaman.2023.106728.

Zhou, S., Zhang, Y., Caylor, K.K., Luo, Y., Xiao, X., Ciais, P., Huang, Y., Wang, G., 2016. Explaining inter-annual variability of gross primary productivity from plant phenology and physiology. Agric. For. Meteorol. 226–227, 246–256. https://doi.org/10.1016/j.agrformet.2016.06.010.